Molecular Immunology 105 (2019) 86–95

Contents lists available at ScienceDirect

Molecular Immunology

journal homepage: www.elsevier.com/locate/molimm

E. coli induced larger neutrophils in the peritoneal cavity of mice with severe septic peritonitis

Yilan Song[a], Guang Yang[b], Zhiqin Li[a], Peiyan Zhao[b], Lei Yang[b], Cuiyun Cui[b], Shiyu Xing[b], Liying Wang[b,*], Yongli Yu[a,**]

[a] Department of Immunology, College of Basic Medical Sciences, Norman Bethune Health Science Center, Jilin University, Changchun, Jilin, China
[b] Department of Molecular Biology, College of Basic Medical Sciences, Norman Bethune Health Science Center, Jilin University, Changchun, Jilin, China

ARTICLE INFO

Keywords:
Neutrophil
E. coli
Septic peritonitis

ABSTRACT

Neutrophils, classified as professional phagocytes, are crucial in killing bacteria and preventing inflammation. When studying the roles of neutrophils in the development of the septic peritonitis induced by *E. coli*, we noticed some of the larger cells existed among peritoneal lavage fluid cells (PLCs). Besides the large size, their nuclei are segmented and flat, and squeezed to the marginal zone of the inner membrane. The cells, therefore, were designated as *E. coli* induced larger neutrophils (e-Neus). Further studies showed that, the e-Neus were ly6G positive, indicating the e-Neus were a type of neutrophils. The enlarged cell size and marginal nucleus of the e-Neus were caused by engulfing abundant of *E. coli*, marking the active participation of the e-Neus in clearance of *E. coli*. Functionally, the e-Neus generated reactive oxygen species (ROS) and IL-10. Furthermore, the occurrence and accumulation of the e-Neus were closely correlated with the severity of septic peritonitis and mortality of the mice. Overall, the e-Neus presented here may enrich the understandings on neutrophil transitions in response to various insults, and could be used to evaluate the severity of septic peritonitis induced by *E. coli*.

1. Introduction

Polymorphonuclear neutrophils (PMN) are the most rapidly and massively recruited innate immune cells to the infection sites where they engulf and kill the invading microorganisms directly (Nathan, 2006). Under physiological conditions, most of the neutrophils are stored at the bone marrow (BM) reserve pool and undergo complete maturation in the pool (Douglas, 2009). During maturation, neutrophils in different stages have distinct nucleus, granularity and function (Borregaard, 2010). The neutrophils in different maturation stages are neutrophil precursor cells, myloblasts, myelocytes, metamyelocytes, banded neutrophils, segmented neutrophils and hypersegmented neutrophils, subsequently. The myloblasts are unipotent stem cells with large and round nucleus relative to the surrounding cytoplasm. The myelocytes have a horseshoe shaped nucleus. The metamyelocytes carry a ring-shape nucleus (Pillay et al., 2013). The banded neutrophils have a curved but not lobular nucleus. The segmented neutrophils are the mature neutrophils with indentations on the nucleus (Borregaard, 2010; Pillay et al., 2013). The hypersegmented neutrophils are the neutrophils with an increased average number of nuclear lobes (Tak et al., 2017).

In bacterial infection, such as *E.coli* induced septic peritonitis (Lorber and Swenson, 1975), numerous neutrophils in different stages could be mobilized from the bone marrow to the peritoneal cavity to eliminate the *E.coli* by phagocytosis, degranulation and neutrophil extracellular traps (NETs) (Mayadas et al., 2014; Silvestre-Roig et al., 2016). During the infection, the *E.coli* may change the morphology and function of the neutrophils. Morphologically, the neutrophils accumulated in the infection site are with segmented nucleus and become larger and less granular. The occurrence of the enlarged neutrophils and the larger immature neutrophils, was demonstrated to be correlated with the increased mortality of mice (van Hout et al., 2015; Seebach et al., 1997). Functionally, during the development of the septic peritonitis, the neutrophils can produce pro-inflammatory mediators, such as TNF-a, IL-1, IL-6, and IL-8, bacteria-killing reactive molecules, such as nitric oxide (NO) and reactive oxygen species (ROS) (Hoesel et al.,

Abbreviations: The e-Neus, the *E. coli* induced larger neutrophils

* Corresponding author at: Department of Molecular Biology, College of Basic Medical Sciences, Norman Bethune Health Science Center, Jilin University, Changchun, 130021, China.
** Corresponding author at: Department of Immunology, College of Basic Medical Sciences, Norman Bethune Health Science Center, Jilin University, Changchun, 130021, China.
E-mail addresses: wlying@jlu.edu.cn (L. Wang), ylyu@jlu.edu.cn (Y. Yu).

https://doi.org/10.1016/j.molimm.2018.11.010
Received 25 May 2018; Received in revised form 23 October 2018; Accepted 14 November 2018
Available online 27 November 2018
0161-5890/

2005). The lifespan of the neutrophils could be prolonged by the stimuli, including cytokines, pathogen-associated molecular patterns (PAMPs), damage associated molecular pattern molecules (DAMPs) or other environmental factors (Silvestre-Roig et al., 2016). Overall, the neutrophils have been described as the neutrophils with the round, banded, ring-shaped, segmented or hypersegmented nucleus.

Unexpectedly, we noticed that some of the larger cells existed among peritoneal lavage fluid cells (PLCs) from the mice with septic peritonitis induced by i.p. injecting big amount of *E. coli*, and the nucleus of the larger cells were segmented and flat, and squeezed to the marginal zone of the inner membrane. The cells were designated as *E. coli* induced larger neutrophils (e-Neus). The aim of this study was to identify the e-Neus, explore their functions and find the correlation of the e-Neus occurrence with the development of bacterial septic peritonitis.

2. Materials and methods

2.1. Antibodies and reagents

APC rat anti-mouse ly6G antibody (560599), FITC rat anti-mouse ly6G antibody (551460), APC-Cy7 rat anti-mouse TNF-α antibody (557644), PE rat anti-mouse IL-10 antibody (561060) were purchased from BD bioscience (Franklin Lakes, NJ, USA). Alexa Fluor® 594 anti-mouse ly6G antibody (clone 1 A8, 127636) was purchased from Biolegend (San Diego, CA, USA). Rabbit anti-mouse IL-10 (ab9969) antibody was purchased from abcom (Cambridge, MA, USA), Alexa Fluor® 488 Conjugate anti-rabbit IgG (4412S) antibody and DAPI (564907) was purchased from Cell Signaling technology (CST; Danvers, MA, USA). Histoque-1119 (11191) and 1077 (10771), dihydrorhodamine123 (DHR; 901464) were purchased from Sigma (St. Louis, MO, USA). Brefeldin A (BFA) were purchased from Beyotime Biotechnology (Shanghai, China). Cell climbing slices (size 14 mm; YA0350) were from Solarbio (Beijing, China). D-Galactosamine hydrochloride (D-galactosamine HCL, DGalN) was purchased from DeBioChem (Nanjing, China). CpG ODN (5′-TCCATGACGTTCCTGAC GTT-3′) was synthesized by Takara Co (Dalian, China). Starch (840621) was purchased from Sinopharm (Beijing, China). Trizol reagent (NC0301) was from Invitrogen (Carlsbad, CA, USA). The cDNA synthesis kit (I21021) and two-step SYBR green qPCR reagent (G31227) were from Transgen (Biotech, Beijing, China). Thioglycollate was purchased from Biotopped Life Science (Beijing, China). *Staphylococcus aureus* were obtained from Pathogenic Microorganism Laboratory, Jilin University.

2.2. E. coli strain and preparation of E. coli culture

E. coli strain JM109 or GFP-expressing *E. coli* (provided by Molecular Biology and Immunology lab, Jilin University) was recovered from freeze-dried powder by being inoculated into a LB medium, and then placed on the agar culture at 37℃ overnight. Single colony was selected to be used as the original strain seed of *E. coli*. The strain seed was picked up and cultured in the 5 mL LB medium at 37℃, 200 rpm. 5 or 7 h later, *E. coli* solution was harvested when the OD value (A_{600}) reached 0.7, and then stored at -20℃ with 20% glycerol solution as working seeds. The working seeds of the *E. coli* were seeded into a new 5 mL LB medium (5%), cultured at 37℃, 200 rpm, till the OD value reached 0.7 and tested the colony forming units (CFUs) (Chen et al., 2003). The CFUs of the *E. coli* culture were calculated and determined as approximately 0.8×10^8 CFUs/mL. For animal experiment use, the *E. coli* pellet after centrifugation at 4000 *g* for 5 min was washed twice using sterile 0.9% NaCl (saline) and then suspended with 1 mL of saline to make 0.8×10^8, 1.6×10^8 and 2.4×10^8 CFUs/mL of *E. coli*, respectively.

2.3. Establishment of septic peritonitis

Eight-week-old female ICR mice (19 ± 1 g in weight) were obtained from Experimental Animal Center, Medical College of Norman Bethune, Jilin University, and maintained in microisolator cages under specific pathogen-free conditions. To establish a septic peritonitis mouse model, the mice were injected intraperitoneally (i.p.) with 1 mL of saline containing 0.8×10^8, 1.6×10^8 and 2.4×10^8 CFUs of *E. coli*, respectively. The survival of mice was recorded and clinical manifestations were evaluated as a clinical score (Gobbetti et al., 2014). The clinical score is based on the following 6 clinical manifestations: lethargy, piloerection, tremors, periorbital exudates, respiratory distress and diarrhea. The mice with a clinical score > 3 or ≤ 3 were defined as undergoing severe sepsis or moderate sepsis, respectively. Experimental manipulation of the mice was undertaken in accordance with the National Institute of Health Guide for the Care and Use of Laboratory Animals, and with the approval of the Scientific Investigation Board of Science & Technology of Jilin Province, China.

2.4. Preparation of PLCs and cell counting

To harvest the PLCs, the mice (n ≥ 3 per group) injected i.p. with *E. coli* or PBS were euthanized with 50 mg/kg pentobarbital sodium at designed time points. The PLCs were collected by washing of peritoneal cavities using 6 mL ice-cold PBS per mouse.

To count the e-Neus in each peritoneal lavage sample, the cells from the samples were harvested by centrifuging at 750 g for 5 min at 4 ˚C and fixed on the glass slides. The slides were stained with hematoxylin-eosin (HE), and photographed under microscope (Olympus BX53). The cells in 5 fields of the slides were numerated.

2.5. Neutrophils purification and cell culture

To isolate neutrophils from bone marrow (BM) cells of naïve mice, the femur and tibia were carefully removed from the euthanized mice. The epiphyses of the bones were cut off, and BM cells were flushed using a 25-gauge needle and a 12 cc syringe with RPMI 1640 supplemented with 10% (V/V) fetal bovine serum (GIBCO) (FBS) and 2 mM EDTA. The BM neutrophils were separated on a density gradient centrifugation (Swamydas and Lionakis, 2013) using Histoque-1119 and 1007. The isolated BM neutrophils (4×10^6) were maintained in RPMI 1640 supplemented with 10% FBS and antibiotics (100 IU of penicillin/ml and 100 IU of streptomycin/ml), seeded in a 24-well plate (Costar, Cambridge, MA), and cultured with or without 5×10^6 CFUs of *E. coli* for 0, 3, 6, 12 and 24 h in a 5% CO_2-humidified incubator at 37 ˚C. The cultured BM neutrophils were collected and centrifuged at 750 *g* for 5 min at 4 ˚C for further use. The neutrophils from PLCs of infected mice and human peripheral blood were also separated by the same methods as mentioned above.

2.6. Immunofluorescent assay

For fluorescent staining, neutrophils (4×10^6) from PLCs of infected mice and BM neutrophils (4×10^6) were cultured with *E. coli* (5×10^6 CFUs) for varied time periods. The cells were fixed with 4% paraformaldehyde (PFA), seeded on the climbing slice in the 24-well plate, attached for 30 min at room temperature, washed twice with PBS supplemented with 1‰ of Triton X-100 (Dingguo Biotechnology, Beijing, China), and blocked with 5% Bovine Serum Albumin (BSA) (Greencore feed science & technology, Guangdong, China) for 1 h at room temperature. Then the cells were stained with Alexa Fluor® 594 Conjugate anti-mouse ly6G (clone 1 A8) mAb (2.5 μg/mL) overnight at 4 ˚C, or with rabbit anti-mouse IL-10 (1 μg/ml) overnight at 4 ˚C overnight, followed by being incubated with 1/1000 Alexa Fluor® 488 conjugate anti-rabbit IgG (2 μg/ml) for 1 h at room temperature. For detecting ROS, the cells were stained with DHR (30 μg/ml) for 5 min at

room temperature. After washing twice with PBS, the cells were counterstained with DAPI (0.5 μg/mL) for 5 min, and then washed. The fluorescent images of the cells were taken under microscope (ZEISS imager. Z2).

2.7. Detection of intracellular TNFα and IL-10 by flow cytometry

For detecting intracellular TNFα and IL-10, the BM neutrophils were cultured with Brefeldin A (BFA) (10 μg/mL) for 3 h, and then collected. The collected cells were stained with fluorescence-conjugated rat anti-mouse ly-6 G antibody for 30 min at room temperature in the dark. The stained cells were fixed with 4% PFA and permeabilized with 0.1% saponin, followed by being stained with fluorescence-conjugated rat anti-mouse TNF-α antibody and rat anti-mouse IL-10 antibody. All stained cells were analyzed by flow cytometry (C6, BD Biosciences).

2.8. Adoptive transfer of anti-Ly6G-labeled BM leukocytes

Freshly isolated BM neutrophils (1.5×10^7) were stained with FITC-conjugated rat anti-mouse ly6G antibody (clone 1 A8) at a concentration of 0.25 μg/million cells in 100 μl PBS plus 2% FBS on ice for 30 min. After washing twice with PBS, the stained neutrophils (1×10^7 in 1 mL PBS) were i.p. injected into recipient mice, followed by i.p. injecting with 2.4×10^8 CFUs of *E. coli* (in 1 mL PBS). After 2 h, the mice were euthanized for collecting PLCs, the PLCs were observed under fluorescent microscope.

2.9. Quantitative real-time polymerase chain reaction

Total RNA was isolated from PLCs with Trizol (Noahcentury, NC0301) and reverse-transcribed using a cDNA synthesis kit (Transgene Biotech, I21021). Quantitative real-time PCR was performed using two-step SYBR green qPCR assays (Transgene Biotech, G31227) and the target genes were identified using the following specific primers: β-actin forward: 5′-GATCAAGATCATTGCTCCTCCTG-3′ and reverse: 5′-AGGGTGTAAAACGCAGCTCA-3′; IL-10 forward: 5′-CAAGGAGCATT TGAATTCCC-3′ and reverse : 5′-GGCCTTGTAGACACCTTGGTC-3′; TNF-α forward: 5′-CTTCTGTCTACTGAACTTCGGG-3′ and reverse: 5′-CACT TGGTGGTTTGCTACGAC-3′. The forward and reverse primers were designed to flanks different exons of the targeted transcript to prevent amplification of genomic DNA. The data were acquired using the Step One real-time PCR system (Applied Biosystems, Foster City, CA, USA). The amplification conditions used were as follows: one cycle at 95 °C (30 s), followed by 40 cycles at 95 °C (5 s) and 64 °C (31 s). Data were normalized to β-actin transcript levels.

2.10. Statistical analysis

Comparisons between groups were conducted using analysis of unpaired t tests. P value < 0.05 (95% confidence interval) was considered to be statistically significant. Statistics were analyzed using GraphPad Prism 5.0 for Windows.

3. Results

3.1. Occurrence of the E. coli induced larger neutrophils

In our previous studies, we noticed the existence of 20% of abnormal “giant cells” in the peritoneal lavage fluid cells (PLCs) in the septic peritonitis mouse induced by *Escherichia coli (E. coli)* intraperitoneally (i.p.) 18 h post-infection (Ren et al., 2016). The “giant cells” were larger than the regular neutrophils with lobulated nucleus which was squeezed to the marginal zone of the inner cell membrane. Comparatively, the regular neutrophils have segmented nucleus or ring-shaped nucleus (Fig. 1A). Morphologically, the “giant cells” resemble the neutrophils relative to their segmented nuclei, but, distinct from the regular neutrophils relative to their size and nucleus distribution. To identify whether the “giant cells” were developed from the neutrophils in response to *E. coli* infection, we infected ICR mice by i.p. injection with 2.4×10^8 CFUs of *E. coli* for 18 h, and then collected the PLCs. The PLCs were stained with hematoxylin-eosin (HE) and observed under microscope (Ren et al., 2016). In the PLCs, approximate 20% of “giant cells” were also found. The “giant cells”, with an average size about 10 μm, are obviously larger than regular neutrophils (5 μm in size) (Fig. 1A). The PLCs were next subjected to the density gradient centrifugation. The cells in the layers marked with M and G in Fig. 1B were harvested and stained with HE. The harvested cells from the G layers consist of 23% “giant cells”. The “giant cells” were further stained with anti-mouse ly6G (clone 1 A8) antibody recognizing the ly6G, a specific surface marker for murine neutrophils (Pillay et al., 2013). Evidently, all “giant cells” were ly6G positive (Fig. 1C) and therefore were designated as *E. coli* induced larger neutrophils (e-Neus). To compare the differences between the e-Neus and the regular neutrophils microscopically, we i.p. injected mice with 2.4×10^8 CFUs of “green” *E. coli* engineered with GFP encoding gene, collected the PLCs at 18 h post-infection and observed. Under fluorescent microscope, we found 38.8% of neutrophils engulfed “green” *E. coli* among the 51% of neutrophils in the total PLCs. Of which, all of the e-Neus and only 4% of regular neutrophils were “green”. Numerically, the e-Neus consumed more “green” *E. coli* than regular neutrophils (Fig. 1D). Under transmission electron microscope (TEM), compared to the regular neutrophils (Fig. 1E), the e-Neus (1) displayed enlarged size with a diameter of 10 μm, while regular neutrophil was 6 μm; (2) contained very few surface ruffles; (3) lost most/all of the granules; (4) internalized plenty of *E. coli* which remained intact or being degraded; (5) formed a large vacuole filled with *E. coli* that squeezed the nucleus close to the inner membrane, whereas, phagosome in regular neutrophil tightly fitting around each bacterium (Fig. 1E). These observations indicated that the e-Neus in the PLCs from mice with septic peritonitis induced by *E. coli* were the enlarged neutrophils.

3.2. Dosage effect of E. coli on the severity of septic peritonitis and occurrence of e-Neus

To determine the relationship between the amount of *E. coli* and the severity of septic peritonitis, we i.p. injected mice with 0.8×10^8, 1.6×10^8 and 2.4×10^8 CFUs of *E. coli* to induce septic peritonitis in the female ICR mice (7 in each group), respectively, and then monitored their physical conditions and recorded the survival. A clinical score (Gobbetti et al., 2014) was used to evaluate the clinical manifestations and the septic peritonitis severity. The result showed that, one hour post-infection, all mice infected began to lassitude, and 3 h later, underwent with or without periorbital exudates and diarrhea. 8 h post-infection, 5 out of 7 mice received 2.4×10^8 CFUs of *E. coli* manifested at least 4 symptoms including lethargy, piloerection, periorbital exudates and diarrhea, indicating the development of severe septic peritonitis (score > 3). On the contrary, the mice received 0.8×10^8 and 1.6×10^8 CFUs of *E. coli* developed moderate sepsis (score ≤ 3), only manifested symptoms of lassitude, periorbital exudates and diarrhea (Fig. 2B). 13 h after infection, the mice received 2.4×10^8 CFUs of *E. coli* displayed respiratory distress, tremors and died at 14 h post-infection. At 24 h, only 2 mice survived (Fig. 2A). However, the mice received 1.6 and 0.8×10^8 CFUs of *E. coli* all survived and did not display any symptoms at 24 h post-infection. Hence, *E. coli,* at a high dose such as 2.4×10^8 CFUs, could induce fatal peritonitis in mice.

Furthermore, we observed the occurrence of e-Neus relative to the severity of peritonitis induced by *E. coli*. The PLCs collected from the mice infected with 0.8×10^8, 1.6×10^8 and 2.4×10^8 CFUs of *E. coli* for 4, 8 and 12 h, were HE stained, and examined under microscope. As expected, we did observe 19%, 25% and 15% or 6%, 5% and 4% of the e-Neus in the PLCs from the mice received 2.4×10^8 or 1.6×10^8 CFUs

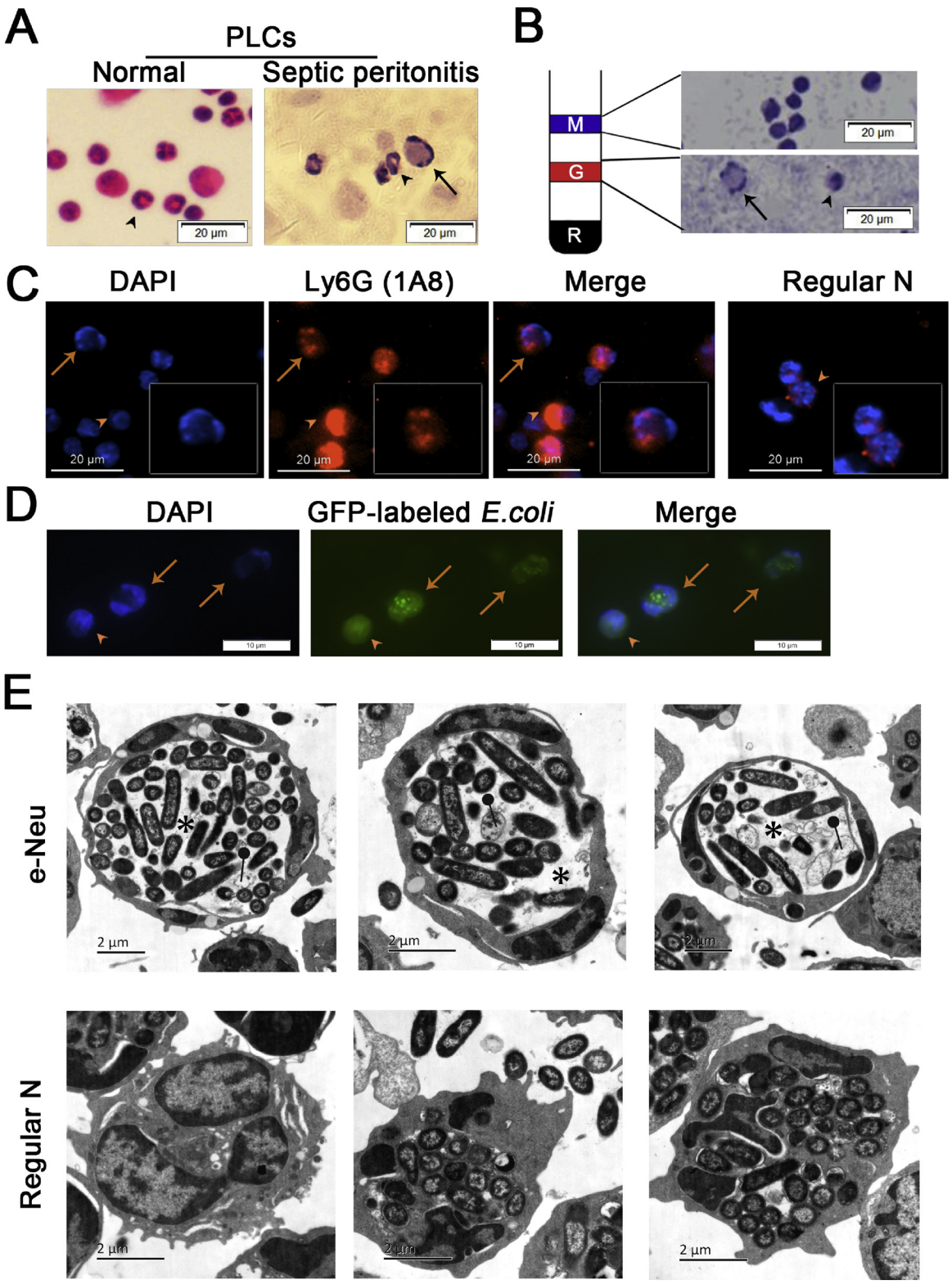

Fig. 1. Morphology of the e-Neus induced by *E. coli* in the peritoneal cavity of mice. ICR mice were i.p. injected with or without 2.4×10^8 CFUs of *E. coli* or GFP-expressing *E. coli* to induce septic peritonitis. After 18 h, PLCs were collected, stained with HE and observed for e-Neus under microscope **(A)**. The PLCs collected were separated by density gradient centrifugation. The cells in the M, G layers were collected separately, stained with HE and observed **(B)**. Mononuclear cells, granulocytes and red blood cells were mainly distributed in M, G, R layers, respectively. The granulocytes collected from the G layer were stained with Alexa Fluor® 594 anti-mouse ly6G (clone 1 A8) (red, middle) and DAPI (blue, left), then observed under fluorescent microscope **(C)**. The e-Neu and the regular neutrophil were shown in the insets. The collected PLCs from mice injected with GFP-expressing *E. coli* were observed under fluorescent microscope **(D)**. The collected PLCs were observed under TEM **(E)**. Arrows, arrowheads, asterisks or lollipops denote the e-Neus, regular neutrophils, spacious vacuoles or degraded *E. coli*, respectively. The experiments were repeated three times. (For interpretation of the references to colour in this figure legend, the reader is referred to the web version of this article.).

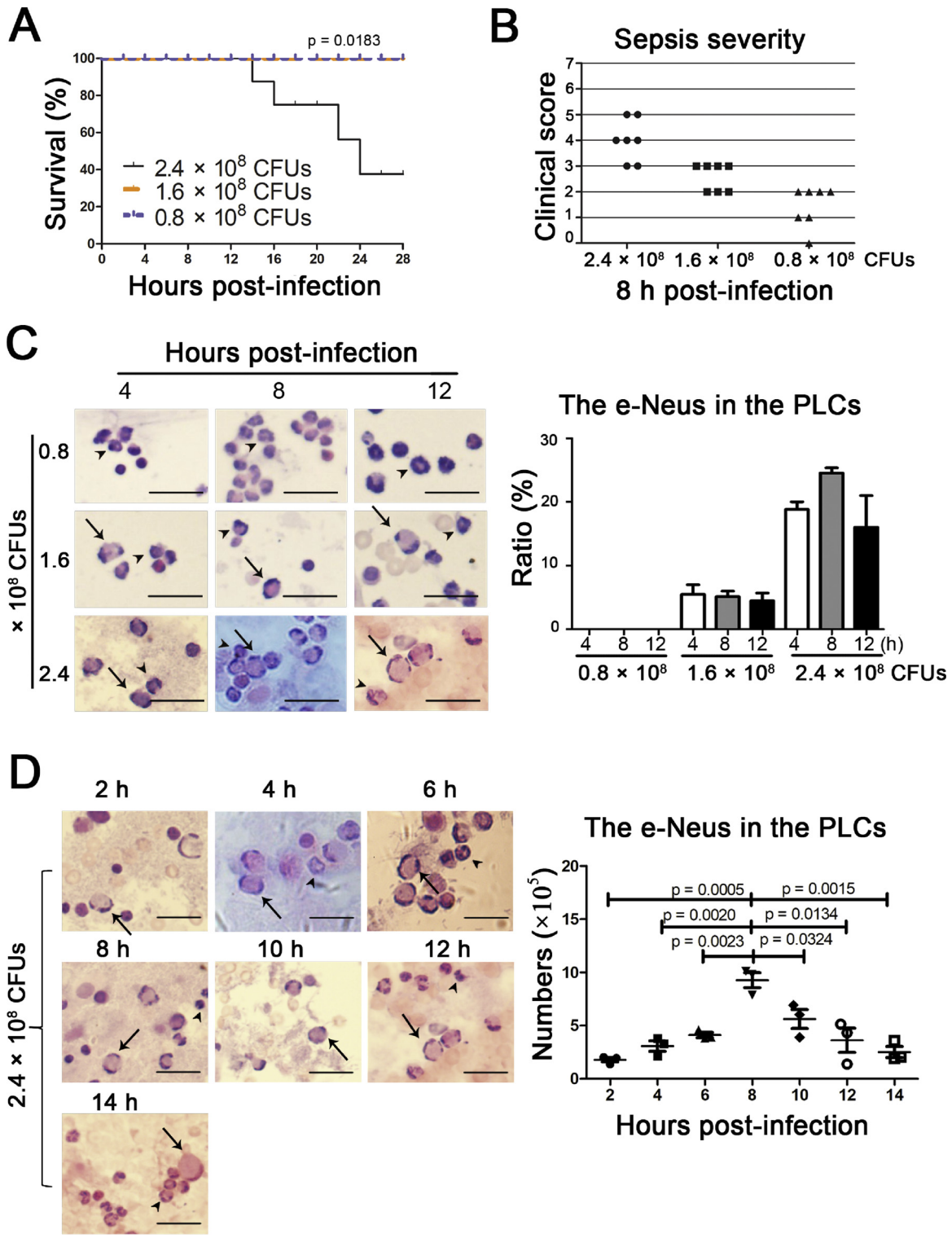

Fig. 2. Mortality of *E. coli*-induced mice and the occurrence of e-Neus in their PLCs. Mice (n = 7) were i.p. injected with *E. coli* at 0.8, 1.6 or 2.4 × 10^8 CFUs of *E. coli* and then recorded their survivals **(A)** and clinical manifestations including lethargy, piloerection, tremors, periorbital exudates, respiratory distress, and diarrhea. The clinical scores **(B)** were obtained based on the clinical manifestations at 8 h post-*E. coli* infection. The PLCs collected from infected mice were stained with HE and numerated for the e-Neus **(C)**. The PLCs from the mice infected with 2.4 × 10^8 CFUs of *E. coli* were collected at 2, 4, 6, 8, 10, 12 and 14 h post-infection, then stained with HE and numerated for the e-Neus **(D)**. Scale bars = 20 μm. Data are represented as mean ± SEM. These experiments were repeated three times.

of *E. coli*, respectively (Fig. 2C). In contrast, no e-Neus were observed in the PLCs from the mice received 0.8 × 10^8 CFUs of *E. coli*. Next, we kinetically observed the occurrence of e-Neus in the mice received 2.4 × 10^8 CFUs of *E. coli* at 2-hour intervals over 14 h, and found that the e-Neus began to occupy 13% of the PLCs (1.77 × 10^5) at 2 h post-infection, timely increased afterwards, reached 25% of the PLCs (9.25 × 10^5) at 8 h, and declined over time. At 14 h, only 5% (2.50 × 10^5) of the e-Neus left (Fig. 2D). Together, these results reveal that the e-Neus could be massively induced in the peritoneal cavity of the mice infected with higher dose of *E. coli*, and their occurrence was

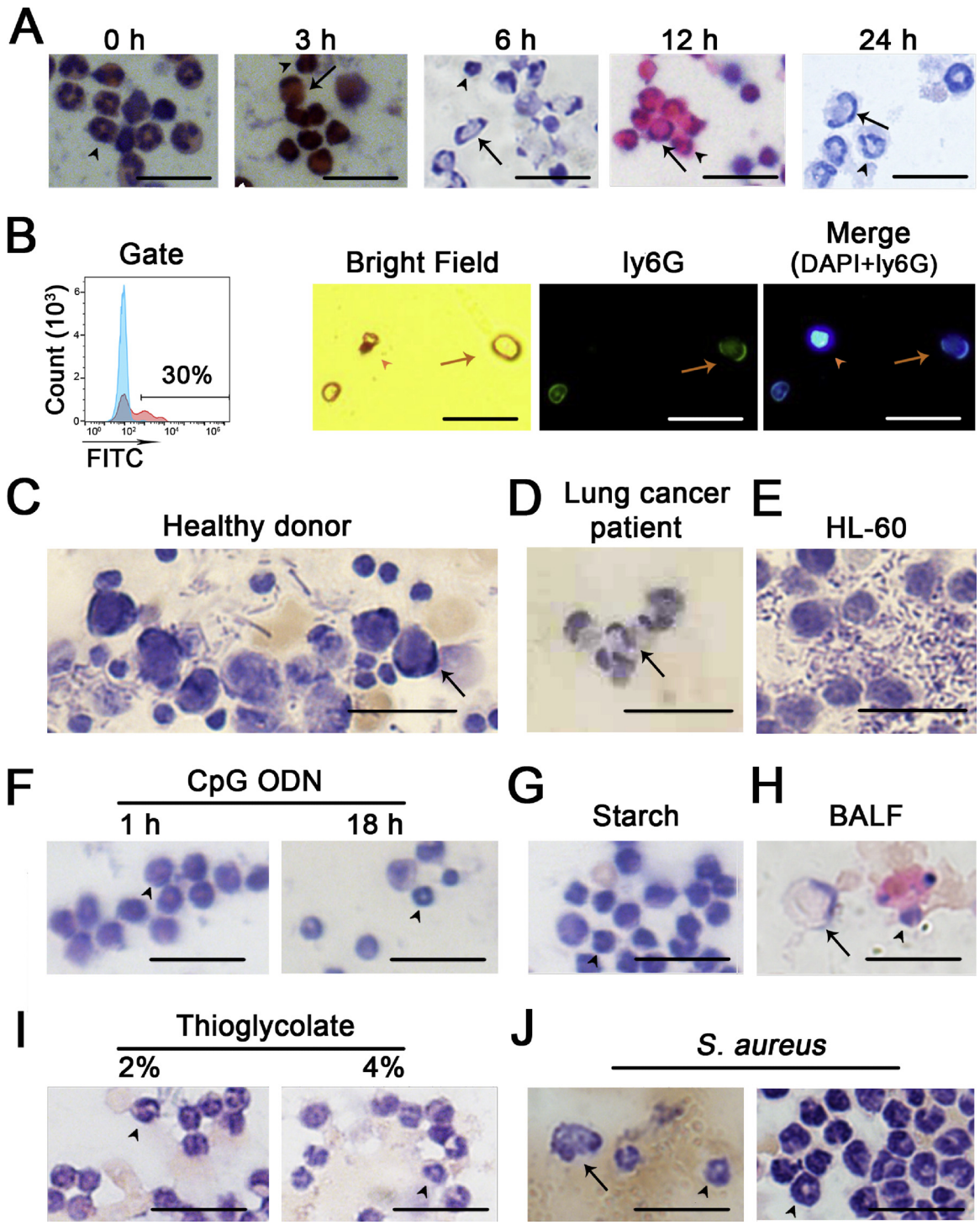

Fig. 3. The induction of the e-Neus *in vivo* and *in vitro*. Isolated murine BM neutrophils (4×10^6) were cultured with 5×10^6 CFUs of *E. coli* for 3, 6, 12, 24 h, and then stained with HE for observing the e-Neus **(A)**. The BM neutrophils (1×10^7) were labeled with FITC rat anti-mouse ly6G antibody, and then were i.p. injected into the mice. After the injection, the mice were i.p. injected with 2.4×10^8 CFUs of *E. coli*. 2 h later, the PLCs were collected and observed under fluorescent microscope **(B)**. Alternatively, human peripheral blood neutrophils from a healthy donor **(C)** or a lung cancer patient **(D)** were cultured with 5×10^6 CFUs of *E. coli* for 6 h, stained with HE, and observed. HL-60 cells (4×10^6), human promyelocytic leukemia cell line cells, were cultured with 5×10^6 CFUs of *E. coli* for 6 h and stained with HE **(E)**. CpG ODN **(F)**, starch **(G)**, thioglycollate **(I)** or *S. aureus* (J) were i.p. injected into the mice. 8 h later, the PLCs were collected, stained with HE and observed. Arrows and arrowheads denote the e-Neus and regular neutrophils, respectively. One of three experiments was represented. Scale bars = 20 μm.

seemingly correlated with the casualties of the mice.

3.3. Elements of driving the e-Neus development

Upon the ly6G expression and the segmented nucleus of the e-Neus, we speculate that the e-Neus were developed from the regular neutrophils, and tried to observe whether the development could also occur *in vitro*. Firstly, we seeded the bone marrow (BM) neutrophils purified from mice in the 24-well plate, 4×10^6 each well, added 5×10^6 CFUs of *E. coli* to infect them, then retrieved cells at 3, 6, 12 and 24 h post-

infection, and observed their morphology and numerated the e-Neus. We found that the e-Neus occupied 60% of the neutrophils at 6 h post-infection, 20% or less than 1% at 12 or 24 h post-infection (Fig. 3A). To trace the development of e-Neus, we labeled freshly isolated BM neutrophils (1×10^7) with FITC-conjugated rat anti-mouse ly6G antibody, and transferred them into the peritoneal cavity of mice, and then mice were infected with 2.4×10^8 CFUs of *E. coli*. After 2 h, the PLCs were retrieved, analyzed and observed. The analysis of flow cytometry showed ly6G positive neutrophils occupied approximately 30% of the total PLCs (Fig. 3B left). Under fluorescent microscope, the enlarged e-Neus were observed with "green" fluorescence (Fig. 3B), signifying ly6G-positive BM derived neutrophils. Thus, the result indicated that the regular neutrophils could be induced to develop into the e-Neus in the peritoneal cavity, in response to massive *E. coli*.

To determine whether the e-Neus could also develop from human neutrophils in response to severe infection of *E. coli in vitro*, we cultured human neutrophils or the HL-60 cells with *E. coli* (5×10^6 CFUs) for 6 h. The neutrophils were isolated from peripheral blood of a healthy donor or a lung cancer patient. The HL-60 cells are human derived neutrophil-like cell line cells. Like that happened in the murine neutrophils, 30% of the e-Neus were seen in the infected neutrophils from the healthy donor (Fig. 3B) and the lung cancer patient (Fig. 3C), and no e-Neus were seen in the HL-60 cells (Fig D). Curiously, we also observed whether the e-Neus could be induced by "non-*E. coli* elements", including CpG ODN, starch, thioglycollate influenza A virus and *Staphylococcus aureus* (*S. aureus*). The CpG ODN (10 μg/per mouse in 300 μl of PBS) was i.p. injected into the mice which were sensitized with D-GalN (0.01 g/g body weight in 500 μl of PBS) for 1.5 h to induce systemic inflammatory response syndrome (SIRS) (Meng et al., 2017). 1 h or 18 h later, the PLCs were collected for observing the e-Neus and were found no e-Neus (Fig. 3E). Also, starch (0.04 g) and thioglycollate (2%, 4%), two typical inducers of aseptic peritonitis, were i.p. injected (both in the 1 mL PBS) into the peritoneal cavity. After 8 h, the PLCs were collected, stained with HE, observed under light microscope, and found no e-Neus (Fig. 3F, G, I). Differently, FM1 virus, a mouse adaptive H1N1 influenza A virus, when intranasally administrated to mice, induced only 2% of the e-Neus in bronchoalveolar lavage fluid (BALF) cells collected on day 7 post infection (Fig. 3G). To validate whether "non-*E. coli* bacteria" could also induce the e-Neus, we i.p. injected mice ($n = 7$) with 2.4×10^8 CFUs of *S. aureus*, then recorded the survivals and collected PLCs followed by HE staining. Infected mice started dying at 4 h post-infection, died mostly except one mouse within 12 h. Given the maximum rate of the e-Neus at 8 h post *E. coli* infection, we collected PLCs after 8 h of *S. aureus* infection. Resultantly, we found that neutrophils accumulated in the peritoneal cavity were 2 fold more than that of *E. coli*, approximate 5×10^6, however, the e-Neus were less than 1% (Fig. 3J). Finally, our results imply that the e-Neus were evidently induced by *E. coli* from the mouse and human neutrophils, barely induced by influenza virus, *S. aureus* and couldn't be induced by un-infectious elements, such as CpG ODN, thioglycollate and starch.

3.4. Functional exploration of the e-Neus

To know whether the e-Neus could produce pro- and anti-inflammatory cytokines, we purified neutrophils from murine BM and tested the production of IL-6, TNF-α and IL-10 in the e-Neus. The purity of the neutrophils was > 92.2% (Fig. 4A). The purified neutrophils were seeded in a 24 well-plate, 4×10^6 per well, incubated with or without 5×10^6 CFUs of *E. coli* for 3, 6 and 12 h, and harvested for detecting their expression of IL-6, TNF-α and IL-10. As shown in Fig. 4B, the *E. coli* challenge significantly induced expression of IL-10 mRNA ($p < 0.05$) at 6, 12 h, elevated the expression of TNF-α mRNA ($p < 0.05$) at 12 h, and induced no obvious elevation of IL-6 mRNA. Next, to examine the protein levels of IL-10 and TNF-α in the e-Neus, we cultured BM neutrophils with GFP-expressing *E. coli* for 3, 6 and 12 h, respectively. The cells were collected and stained with fluorescence-labeled anti-ly6G, anti-IL10 and anti-TNF-α mAb, and analyzed by flow cytometric assay. Firstly, we gated the $ly6G^+$ neutrophils (Fig. 4C). The gated cells were further analyzed in gate P1, P2 and P3, respectively. The neutrophils in gate P1, P2 and P3 displayed no fluorescence ("$green^{negative}$"), less fluorescence ("$green^{low}$") or high fluorescence ("$green^{high}$"), representing "$green^{negative}$", "$green^{low}$" or "$green^{high}$" neutrophils, also representing neutrophils which engulfed no, less or more GFP-expressing *E.coli*, respectively. Based on the observations (Fig. 1D) that all of the e-Neus, after consuming abundant of GFP-expressing *E. coli*, were enlarged and "green" under the fluorescence microscope, while only 4% of regular neutrophils were "green", even though the neutrophils exposed to the same amount of GFP-expressing *E. coli*, therefore, we gated the $ly6G^+$ "$green^{high}$" neutrophils to roughly represent the e-Neus for detecting their expression of IL-10 and TNF-α. Intriguingly, the "$green^{high}$" neutrophils obviously increased the production of IL-10 post *E. coli* challenge at 3, 6, 12 h, in contrast, barely increased the production of TNF-α (Fig. 4C). To identify, we cultured mouse BM neutrophils with *E. coli* for 6 or 12 h, and then dropped the cells onto glass coverslips for intracellular staining with fluorescent antibodies against IL-10. As shown in Fig. 4D, the e-Neus were intensely stained with the IL-10 antibody. In comparison, the IL-10 level in the e-Neus was far lower than that of regular neutrophils. Quantitative analysis by mean optical density (MOD) further showed that the IL-10 was 1/4 fold less ($p < 0.05$) expressed in the e-Neus than that of regular neutrophils at 6 h post *E. coli* challenge. Thereby, the e-Neus were IL-10 producing neutrophils.

In response to bacteria, neutrophils produce reactive oxygen species (ROS) which kill off pathogens, cause tissue damage, and participate in the inflammatory resolution (Hoffmann & Griffiths, 2018). To validate whether the e-Neus could also produce ROS, we cultured BM neutrophils with *E. coli* for 6 or 12 h. The cells were then stained with dihydrorhodamine (DHR) (30 μg/ml) for 5 min, and observed under the fluorescent microscope. The e-Neus, as shown in Fig. 4E, emitted green fluorescence as the regular neutrophils did. Comparatively, the fluorescent intensity of the e-Neus was remarkably lower than that of regular neutrophils (Fig. 4E). The observation indicated that the e-Neus were ROS generating neutrophils.

4. Discussion

Here, we described the discovery of the e-Neus which were found in the PLCs of the mice with severe *E. coli* infection. The e-Neus were identified as $ly6G^+$ neutrophils with enlarged cell size and lobulated nucleus located to the inner side of cell membrane. The origin of the e-Neus was also confirmed by transferring ly6G antibody labeled neutrophils into the peritoneal cavity of the mice infected with massive *E. coli*. The occurrence of the e-Neus could be "*E.coli*-specific" because the "non-bacterial elements", such as CpG ODN, starch, thioglycolate or FM1 influenza virus, or "non-*E.coli* bacteria", such as *S. aureus*, another common peritonitis causing bacterium, failed to induce or only induced a few e-Neus, although, they all induced intensive infiltration of the neutrophils in the peritoneal cavity. In the *in-vitro* setting, the e-Neus were also induced from the mouse BM neutrophils and human peripheral blood neutrophils (PBNs) by culturing the cells with *E. coli* (5×10^6 CFUs). Thus, the e-Neus could be considered as a type of specialized neutrophils induced by *E.coli*. Their occurrence could signify the desperate fighting with *E. coli* and the severity of *E. coli* caused septic peritonitis.

To our knowledge, the e-Neus were a type of larger neutrophils occurred in physiological or pathological conditions and different from the previously described larger neutrophils, such as "hybrid" neutrophils, giant neutrophils and larger, less granular neutrophils (LL-Ns). "Hybrid" neutrophils were induced from mouse BM neutrophils cultured with granulocyte macrophage colony-stimulating factor (GM-CSF), IFN-γ, TNF-α or IL-4, being characterized by enlarged cell size, formation of podosomes, and oval-shaped nuclei (Matsushima et al.,

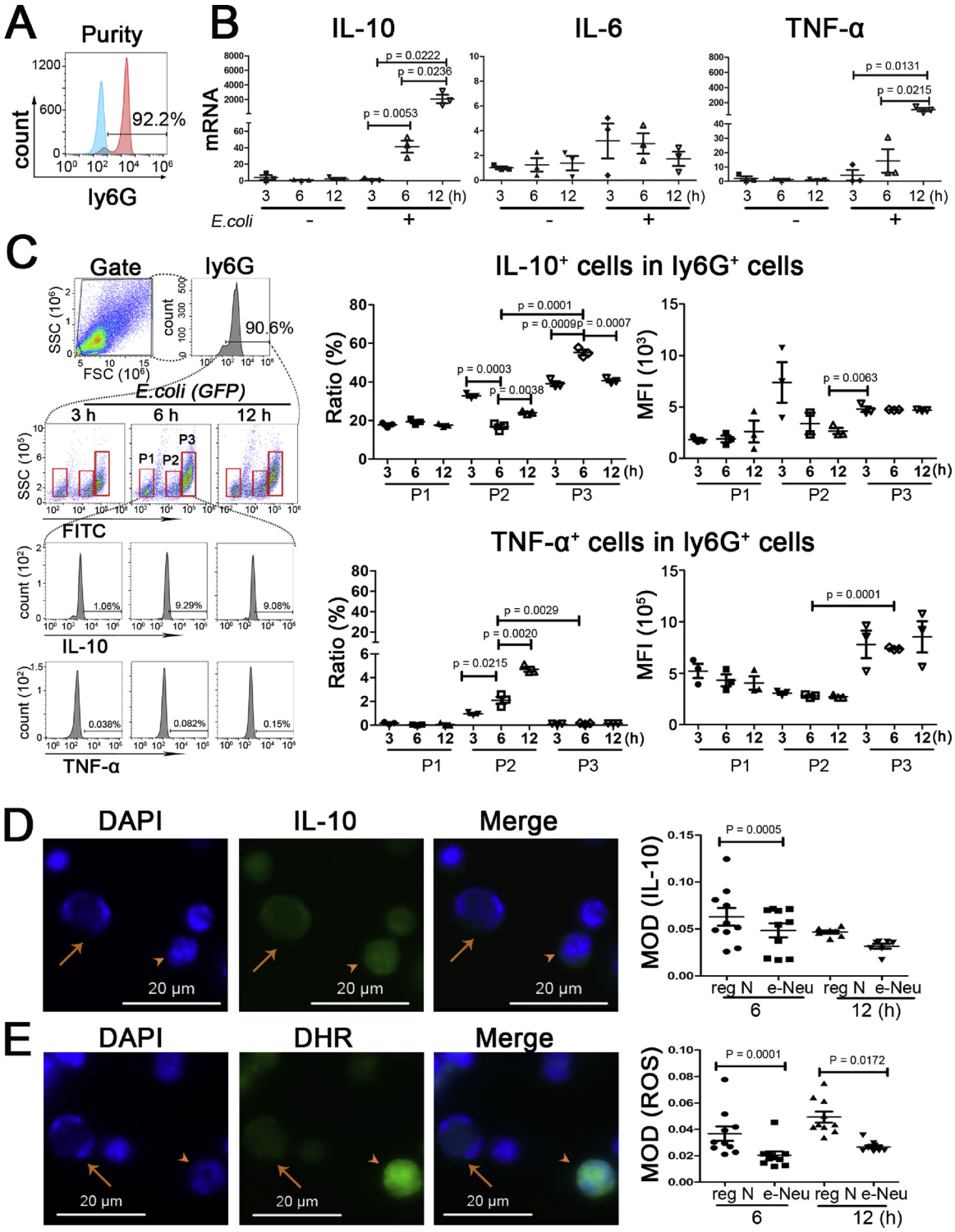

Fig. 4. Detection of inflammatory cytokines and ROS in the *E. coli*-treated BM neutrophils *in vitro*. **(A)** Purity of the BM neutrophils. The freshly isolated BM neutrophils were stained with fluorescent Ly6G mAb, and analyzed by flow cytometry. **(B)** The mRNA levels of IL-10, IL-6 and TNF-α in the purified BM neutrophils. BM neutrophils were cultured with *E. coli* for 3, 6, 12 h and then used for detecting IL-10, IL-6 and TNF-α mRNA by quantitative real time PCR. **(C)** The protein levels of IL-10 or TNF-α in the ly6G$^+$ neutrophils. Isolated BM neutrophils were cultured with GFP-expressing *E. coli* for 3, 6, 12 h, stained with fluorescent Ly6G, IL-10, TNF-α mAbs, and analyzed by flow cytometry. P1, P2 and P3 denote the gates for the Ly6G$^+$ neutrophils with no green fluorescence, less green fluorescence or high green fluorescence, respectively. **(D)** Production of IL-10 in BM neutrophils. BM neutrophils were cultured with *E. coli* for 6, 12 h, stained with rabbit anti-mouse IL-10 mAb, followed with fluorescent anti-rabbit IgG, and then observed under fluorescent microscope. The IL-10 protein level in the cells was represented by mean optical density (MOD). **(E)** Production of ROS in BM neutrophils. BM neutrophils were cultured with *E. coli* for 6, 12 h, stained with dihydrorhodamine (DHR) (30 ug/ml), and then observed under fluorescent microscope. The ROS level in the cells was represented by MOD. Reg N indicates regular neutrophils. Arrows and arrowheads denote the e-Neus and regular neutrophils. Data are represented as mean ± SEM (For interpretation of the references to colour in this figure legend, the reader is referred to the web version of this article.).

2013; Takashima and Yao, 2015). Giant neutrophils were observed among the isolated human peripheral neutrophils cultured for 7 days, without adding external cytokines or growth factors. Morphologically, they are large vacuolated cells with a round nuclei, and the presence of large phagosomes enclosing neutrophil granules in the cytoplasm (Dyugovskaya et al., 2014; Zonneveld et al., 2016). LL-Ns are a type of septic neutrophils occurred in the sepsis patient blood with other types of septic neutrophils including mature neutrophils and immature neutrophils (larger) (Mardi et al., 2010). Of note, the e-Neus are distinct from others in morphology, including size, shape of nucleus, composition.

Comparatively, the e-Neus (10 μm) are larger than the regular mature neutrophils (5 μm) in the peritoneal cavity from sepsis mice, and much smaller than LL-Ns (16.2 μm), "hybrid" neutrophils (22 μm) or giant neutrophils (50 μm) (Dyugovskaya et al., 2014), respectively. The enlargement of the e-Neus could be attributed to degranulation and membrane addition in response to the *E. coli*. The presumption could be supported by the evidences that *E. coli* stimulate degranulation of human neutrophils as early as 5 s after incubation (Pryzwansky et al., 1979), and the degranulation in human neutrophils enlarges the cells by inducing fusion of granule membranes and cell membrane (HOFFSTEIN, 1982). As shown in Fig. 1A, the nucleus of e-Neus is segmented, flat, and squeezes closed to the inner cell membrane, making the e-Neus distinguished from other reported larger neutrophils. The nucleus of the giant cells (Dyugovskaya et al., 2014) is round and inclined towards the cell membrane. The "hybrid" neutrophils are with an oval-shaped nucleus (Matsushima et al., 2013), and LL-Ns with segmented nucleus (Mardi et al., 2010).

Furthermore, although the lobulated nuclei of the e-Neus resembled them as mature neutrophils (Douglas, 2009), the e-Neus, however, were somehow disparate from the reported the mature neutrophils. As shown in Fig. 1E, the e-Neus engulfed much more abundant *E. coli* than the regular neutrophils, among which existed approximate 20% of mature neutrophils characterized by segmented nuclei (Douglas, 2009), implying that the e-Neus might upregulate the phagocytosis-related receptors on their surface. The implication could be supported by the evidence that upregulation of the complement receptor type 3 (CR3) increased the phagocytotic ability of the neutrophils (Mittal et al., 2010), and that the expression of TLR4, CR1 (CD35) and Mac-1 (CD11b/CD18) were relevant to the phagocytosis of the neutrophils (Chen et al., 2014; Underhill and Ozinsky, 2002; Urbaczek et al., 2014). Unlike mature neutrophils that packed the *E. coli* in a "tight" phagosome, the e-Neus packed the *E. coli* in a "spacious" phagosome-like vacuole (Fig. 1E). Since the "spacious" vacuole, unlike the "tight" phagosome, was demonstrated to allow survival of packed bacteria (Nazareth et al., 2007), the e-Neus might develop as a type of neutrophils with deficient bactericidal activity after engulfing overwhelming *E. coli*.

Initially, the e-Neus were noticed in the PLCs of the mice with severe *E. coli* infection. The excessive *E. coli* engulfed by the e-Neus, as revealed in Fig. 1 D and E, leading us to speculate that the e-Neus might be resulted from the extravagant phagocytosis of *E. coli*. To confirm this, we tried to induce the e-Neus with other no *E. coli* (1.4–2 μm long, 0.5 μm wide) particles including influenza virus (50 to 120 nm) (Noda, 2011), *S. aureus* (0.7–1.2 μm) (Shimoda et al., 1995) or starch (2–20 μm) (Timgren et al., 2011), all of which are capable of being phagocytized. Resultantly, only sparsely existed e-Neus were induced by influenza virus or *S. aureus*, and no e-Neus were induced by starch, indicating that the phagocytosis, if involved, was not the major inducement of the e-Neus, and other inflammatory elements could contribute to the inducement. To verify this, we used thioglycollate (Liao et al., 1999) and CpG ODN (Zhang et al., 2010), two documented sterile inflammation inducers, to induce the e-Neus, and failed to induce the e-Neus in the peritoneal cavity of the mice i.p. injected with thioglycollate or CpG ODN. Together with the results that *S. aureus* induced few e-Neus and overwhelming inflammation, the inflammation elicited by "non-bacterial elements" or "non-*E. coli* bacteria", might not be the primary cause for the e-Neu induction. Mulling the *E. coli* preference of the e-Neus, we might speculate the existence of *E. coli* unique elements which would be responsible for the transition of the regular neutrophils to the e-Neus. The speculation is worthwhile to be validated in the further studies.

E. coli have been reported to induce neutrophil necrosis, leading to the lytic cell death with leakage of cell contents (Russo et al., 2005). The findings engendered us to suspect that the *E. coli* induced e-Neus were the neutrophils in a circle of the lytic cell death, therefore being enlarged. To verify this, we cultured BM neutrophils with the *E. coli* for 6 h and observed the induced e-Neus by TEM (Fig. 1E), and found that (1) the nucleus of the e-Neus was lobulated and clinged to the cell membrane. The nucleus was different from that of necrotic neutrophils that had only one fused nucleus with a large round structure (Russo et al., 2005); (2) the cell membrane integrity of the e-Neus remained intact. The intactness of the e-Neus was not resembled to that of the necrotic neutrophils with disintegrative membrane, leading to the leakage of cell contents (Bliss-Moreau et al., 2017); (3) the huge single vacuole of the e-Neus contained abundant of intact bacteria. The existence of the intact bacteria denoted the ongoing bacterial digestion by the e-Neus, a process unobservable in the necrotic neutrophils.

Together, the e-Neus induced by *E. coli* for 6 h could be viewed as the alive neutrophils. To follow the fate of the e-Neus, we cultured the BM neutrophils (4×10^6) with *E. coli* (5×10^6 CFUs) for 3, 6, 12, 24 h, and numerated the e-Neus. The numeration showed that 1.088×10^6, 2.098×10^6, 0.389×10^6, 0.009×10^6 of the e-Neus were recorded at 3, 6, 12, 24 h post-induction, respectively, and indicated that the e-Neus were massively induced as early as 3 h, and peaked at 6 h, and then tended to decrease dramatically. Therefore, the data suggested that the e-Neus were rapidly induced by *E. coli* and short-lived neutrophils.

Prospectively, the firstly described e-Neus could be used as an indicator for evaluating the severity of septic peritonitis clinically. Being inspired, we need to investigate whether the e-Neus (1) are only developed from certain subpopulation of regular neutrophils; (2) could occur in the CLP patients; (3) display other phenotype and function; (4) can restore the morphology and function of regular neutrophils.

Conflict of interests

The authors declare that there is no conflict of interest.

Funding

This work was supported by National Natural Science Foundation of China [grant number 81471888].

Acknowledgments

The authors would like to thank Yun Yao for technical assistance and Xiuping Meng, Yue Xiao for analysis strategies.

References

Bliss-Moreau, M., Chen, A.A., D'Cruz, A.A., Croker, B.A., 2017. A motive for killing: effector functions of regulated lytic cell death. Immunol. Cell Biol. 95 (2), 146–151.
Borregaard, N., 2010. Neutrophils, from marrow to microbes. Immunity 33 (5), 657–670.
Chen, C.-Y., Nace, G.W., Irwin, P.L., 2003. A 6×6 drop plate method for simultaneous colony counting and MPN enumeration of Campylobacter jejuni, Listeria monocytogenes, and Escherichia coli. J. Microbiol. Methods 55 (2), 475–479.
Chen, M.L., Wu, S., Tsai, T.C., Wang, L.K., Tsai, F.M., 2014. Regulation of neutrophil phagocytosis of Escherichia coli by antipsychotic drugs. Int. Immunopharmacol. 23 (2), 550–557.
Douglas, S.D., 2009. Phagocyte-pathogen interactions. Microbe 4 (11), 527–528.
Dyugovskaya, L., Berger, S., Polyakov, A., Lavie, L., 2014. The development of giant phagocytes in long-term neutrophil cultures. J. Leukoc. Biol. 96 (4), 511–521.
Gobbetti, T., Coldewey, S.M., Chen, J., McArthur, S., le Faouder, P., Cenac, N., Flower, R.J., Thiemermann, C., Perretti, M., 2014. Nonredundant protective properties of FPR2/ALX in polymicrobial murine sepsis. Proc. Natl. Acad. Sci. U. S. A. 111 (52),

18685–18690.
Hoesel, L.M., Neff, T.A., Neff, S.B., Younger, J.G., Olle, E.W., Gao, H., Pianko, M.J., Bernacki, K.D., Sarma, J.V., Ward, P.A., 2005. Harmful and protective roles of neutrophils in sepsis. Shock 24 (1), 40–47.
Hoffstein, S.T., 1982. Degranulation, membrane addition, and shape change during chemotactic factor-induced aggregation of human neutrophils. J. Cell Biol. 95, 234–241.
Liao, F., Schenkel, A.R., Muller, W.A., 1999. Transgenic mice expressing different levels of soluble platelet/endothelial cell adhesion molecule-IgG display distinct inflammatory phenotypes. J. Immunol. 163 (10), 5640–5648.
Lorber, B., Swenson, R.M., 1975. The bacteriology of intra-abdominal infections. Arch. Surg. 55 (6), 1349–1354.
Mardi, D., Fwity, B., Lobmann, R., Ambrosch, A., 2010. Mean cell volume of neutrophils and monocytes compared with C-reactive protein, interleukin-6 and white blood cell count for prediction of sepsis and nonsystemic bacterial infections. Int. J. Lab. Hematol. 32 (4), 410–418.
Matsushima, H., Geng, S., Lu, R., Okamoto, T., Yao, Y., Mayuzumi, N., Kotol, P.F., Chojnacki, B.J., Miyazaki, T., Gallo, R.L., Takashima, A., 2013. Neutrophil differentiation into a unique hybrid population exhibiting dual phenotype and functionality of neutrophils and dendritic cells. Blood 121 (10), 1677–1689.
Mayadas, T.N., Cullere, X., Lowell, C.A., 2014. The multifaceted functions of neutrophils. Annu. Rev. Pathol. 9, 181–218.
Meng, X., Sun, W., Ren, Y., Xiao, Y., Zhao, P., Lu, W., Hua, L., Wang, L., Wang, L., Yu, Y., 2017. Protective role of surface Toll-like receptor 9 expressing neutrophils in local inflammation during systemic inflammatory response syndrome in mice. Mol. Immunol. 90, 74–86.
Mittal, R., Gonzalez-Gomez, I., Panigrahy, A., Goth, K., Bonnet, R., Prasadarao, N.V., 2010. IL-10 administration reduces PGE-2 levels and promotes CR3-mediated clearance of Escherichia coli K1 by phagocytes in meningitis. J. Exp. Med. 207 (6), 1307–1319.
Nathan, C., 2006. Neutrophils and immunity: challenges and opportunities. Nat. Rev. Immunol. 6 (3), 173–182.
Nazareth, H., Genagon, S.A., Russo, T.A., 2007. Extraintestinal pathogenic Escherichia coli survives within neutrophils. Infect. Immun. 75 (6), 2776–2785.
Noda, T., 2011. Native morphology of influenza virions. Front. Microbiol. 2, 269.
Pillay, J., Tak, T., Kamp, V.M., Koenderman, L., 2013. Immune suppression by neutrophils and granulocytic myeloid-derived suppressor cells: similarities and differences. Cell. Mol. Life Sci. 70 (20), 3813–3827.
Pryzwansky, K.B., Macrae, E.K., Spitznagel, J.K., Cooney, M.H., 1979. Early degranulation of human neutrophils: Immunocytochemical studies of surface and intracellular phagocytic events. Cell 18 (4), 1025–1033.
Ren, Y., Hua, L., Meng, X., Xiao, Y., Hao, X., Guo, S., Zhao, P., Wang, L., Dong, B., Yu, Y., Wang, L., 2016. Correlation of surface toll-like receptor 9 expression with IL-17 production in neutrophils during septic peritonitis in mice induced by E. coli. Mediators Inflamm. 2016, 3296307.
Russo, T.A., Davidson, B.A., Genagon, S.A., Warholic, N.M., Macdonald, U., Pawlicki, P.D., Beanan, J.M., Olson, R., Holm, B.A., Knight 3rd, P.R., 2005. E. coli virulence factor hemolysin induces neutrophil apoptosis and necrosis/lysis in vitro and necrosis/lysis and lung injury in a rat pneumonia model. Am. J. Physiol. Lung Cell Mol. Physiol. 289 (2), L207–216.
Seebach, J.D., Morant, R., Rüegg, R., Seifert, B., Fehr, J., 1997. The diagnostic value of the neutrophil left shift in predicting inflammatory and infectious disease. Am. J. Clin. Pathol. 107 (5), 582.
Shimoda, M., Ohki, K., Shimamoto, Y., Kohashi, O., 1995. Morphology of defensin-treated Staphylococcus aureus. Infect. Immun. 63 (8), 2886–2891.
Silvestre-Roig, C., Hidalgo, A., Soehnlein, O., 2016. Neutrophil heterogeneity: implications for homeostasis and pathogenesis. Blood 127 (18), 2173–2181.
Swamydas, M., Lionakis, M.S., 2013. Isolation, purification and labeling of mouse bone marrow neutrophils for functional studies and adoptive transfer experiments. J. Vis. Exp. (77), e50586.
Tak, T., Wijten, P., Heeres, M., Pickkers, P., Scholten, A., Ajr, H., Vrisekoop, N., Leenen, L.P., Jeam, B., Tesselaar, K., 2017. Human CD62L(dim) neutrophils identified as a separate subset by proteome profiling and in vivo pulse-chase labelling. Blood 129 (26).
Takashima, A., Yao, Y., 2015. Neutrophil plasticity: acquisition of phenotype and functionality of antigen-presenting cell. J. Leukoc. Biol. 98 (4), 489–496.
Timgren, A., Rayner, M., Sjöö, M., Dejmek, P., 2011. Starch particles for food based Pickering emulsions. Procedia Food Sci. 1, 95–103.
Underhill, D.M., Ozinsky, A., 2002. Phagocytosis of microbes: complexity in action. Annu. Rev. Immunol. 20, 825–852.
Urbaczek, A.C., Toller-Kawahisa, J.E., Fonseca, L.M., Costa, P.I., Faria, C.M., Azzolini, A.E., Lucisano-Valim, Y.M., Marzocchi-Machado, C.M., 2014. Influence of FcgammaRIIIb polymorphism on its ability to cooperate with FcgammaRIIa and CR3 in mediating the oxidative burst of human neutrophils. Hum. Immunol. 75 (8), 785–790.
van Hout, G.P., van Solinge, W.W., Gijsberts, C.M., Teuben, M.P., Leliefeld, P.H., Heeres, M., Nijhoff, F., de Jong, S., Bosch, L., de Jager, S.C., Huisman, A., Stella, P.R., Pasterkamp, G., Koenderman, L.J., Hoefer, I.E., 2015. Elevated mean neutrophil volume represents altered neutrophil composition and reflects damage after myocardial infarction. Basic Res. Cardiol. 110 (6), 58.
Zhang, Q., Raoof, M., Chen, Y., Sumi, Y., Sursal, T., Junger, W., Brohi, K., Itagaki, K., Hauser, C.J., 2010. Circulating mitochondrial DAMPs cause inflammatory responses to injury. Nature 464 (7285), 104–107.
Zonneveld, R., Molema, G., Plotz, F.B., 2016. Analyzing neutrophil morphology, mechanics, and motility in sepsis: options and challenges for novel bedside technologies. Crit. Care Med. 44 (1), 218–228.